Four-decade response of ecological risk to land use changes in the Yangtze River Basin

Abstract: Understanding land use/cover change (LUCC) dynamics in the Yangtze River Basin is crucial for effective watershed management and land use policy formulation. Based on land use data from 1980 to 2020 in the Yangtze River Basin, this study used land use analysis models to explore the characteristics and hotspots of LUCC. The geographic detector was applied to identify the driving factors during different periods, and the ecological risk model revealed the evolution of ecological risk across the basin. Results indicate a shift in the dominant drivers of LUCC from socioeconomic factors to natural geographic factors, with an increasing role of multi-factor interactions. Before 2000, the expansion of built-up land and waterbodies dominated changes, whereas frequent mutual conversions among cropland, woodland, and grassland prevailed after 2000. The total area undergoing LUCC after 2000 was 10.2 times larger than before 2000. Approximately 70% of LUCC events involved transitional changes, with the most prominent shifts occurring upstream. Continued land development has increased ecological risk across 3.1×10^4 km^2. Overall, basin-wide land use transitioned from rapid development of available land towards encroachment on ecological land. Complex land type inter-conversions contributed to the clustering of relatively-high-risk and high-risk ecological zones. These findings underscore the necessity for spatially differentiated land management strategies and provide a scientific foundation for sustainable land use planning and ecological risk mitigation in the Yangtze River Basin.

Keywords: Land use/cover change; Transitional land change; Geographic detector; Ecological risk evolution; Yangtze River Basin

1. Introduction

Over the past millennium, humans have altered about three-quarters of the Earth's land surface

(Luyssaert et al. 2014, Winkler et al. 2021). Land use/cover change (LUCC) is one of the most widespread phenomena across global regions and represents the most direct impact of human activities on the Earth's surface system(Vadrevu and Ohara 2020, Yang et al. 2024). LUCC is mainly regulated by human activities and natural factors (Liu et al. 2010, van Asselen and Verburg 2013). Urbanization and population growth are major drivers of LUCC and ecosystem degradation, resulting in forest loss, cropland expansion, desertification, and further impacts on climate and ecosystem functions (Gao and Liu 2011, Lawler et al. 2014). From 1960 to 2019, the total global area affected by LUCC reached approximately 43 million km². LUCC has become a foundational component of large-scale environmental research and a major focus in global change science (Lambin and Meyfroidt 2011, Long 2014, Song et al. 2018). Domestic and international scholars have conducted extensive and in-depth studies on the spatial and temporal patterns of LUCC (Seto and Fragkias 2005, Chen et al. 2006, Deng et al. 2009). Jing et al. (2024) found that global land cover exhibits a latitudinal distribution pattern in mid-latitude regions, while in high- and low-latitude regions, it tends to follow a longitudinal pattern. Ning et al. (2018) revealed that since 2010, LUCC in different regions of China has shown new characteristics, with accelerated expansion of built-up land and cropland loss in central China, and significantly increased expansion of built-up land in western China. Yuan et al. (2023) reported a significant trend of built-up land expansion and cropland loss in the Yangtze River Basin, which became more pronounced after 2000.A general consensus has emerged that LUCC is shaped by both anthropogenic and natural drivers, and that its impacts on ecosystems and environmental risks are profound. However, important divergences remain, particularly regarding the dominant drivers of LUCC in complex regions and the interactions among different land categories. In large-scale basins such as the Yangtze River Basin,

which spans diverse climatic, topographic, and socio-economic zones, the spatiotemporal characteristics and ecological consequences of LUCC are highly heterogeneous and remain insufficiently quantified.

Since the implementation of reform and opening-up policies, significant changes have occurred in land use and land cover across much of China(Yang et al. 2014). The complex interplay of geographic and climatic conditions has contributed to diverse land use patterns, resulting in marked spatial heterogeneity in LUCC across different regions of the country (Yang et al. 2021). Cropland expansion has weakened investments in natural capital (Kong et al. 2023), while large-scale afforestation has become the dominant contributor to China's terrestrial carbon sinks (Yu et al. 2022). Meanwhile, rapid urbanization has led to unprecedented changes in land use, with geographic, climatic, and anthropogenic factors driving LUCC to varying degrees over time (Wu and Hobbs 2002, Serra et al. 2008, Liu et al. 2010). Consequently, quantifying and understanding the spatiotemporal dynamics of LUCC in critical regions is essential for addressing pressing issues such as climate change, biodiversity loss, and food security (Feng et al. 2016, Bayer et al. 2017, Bryan et al. 2018, Chen et al. 2019).

As the third largest river basin in the world, the Yangtze River Basin accounts for about 6% of the global population, and 80% of the land in the basin is suitable for human life. In recent decades, the rapid development of urbanization and industrialization in the Yangtze River Basin has led to a decline in the quality of the ecological environment and the value of ecological services in the region. Land use in the Yangtze River basin is influenced by geographical and climatic factors and social factors basin land types have been drastically changed in a short period of time, most of which is the expansion of construction land and conversion of farmland (Montgomery 2007, Jiang et al. 2012,

Liu et al. 2015, Kong et al. 2018, Yang et al. 2021). Kong et al. (Kong et al. 2018) found that 48% of LUCC in the Yangtze River Basin between 2000 and 2015 was driven by urbanization, confirming it as the primary force behind LUCC in the basin. He et al.(He et al. 2018) also noted that with the acceleration of urbanization, unstable farmland in the basin has undergone significant uphill migration, with an average slope increase of 2.09°.

In contrast, LUCC driven by changes in natural conditions tends to exhibit broader spatial coverage and more persistent impacts, resulting in regionally differentiated land evolution patterns and driving mechanisms within large river basins (Powers and Jetz 2019, Soroye et al. 2020, Kong et al. 2022). Therefore, compared to small-scale regional studies, basin-scale analyses are better suited to capture the geographical heterogeneity of LUCC and to identify the shifting relative contributions of human and natural drivers over long-term land use trajectories. This study aims to reveal the characteristics and spatiotemporal characteristics of LUCC in the Yangtze River Basin, identify the main causes of change by examining variations in the influence of driving factors across different time periods, and clarify the resulting shifts in ecological risk patterns induced by LUCC. This study enhances understanding of the spatiotemporal dynamics of LUCC in the Yangtze River Basin, highlights the interplay of human and natural drivers, and provides valuable insights for ecological risk assessment and integrated watershed management.

2. Methods and materials

2.1. Study area

The Yangtze River flows from west to east across central China (90°~123°E, 24°~36°N), passing through 17 provincial-level administrative regions (Fig. 1). It originates from the Tibetan Plateau, traverses the Sichuan Basin, Dongting Lake Plain, Han River Plain, and finally empties

into the East China Sea at Shanghai. The river has a total length of 6397 km and a watershed area of 1.8 million km^2. Most of the basin falls within a subtropical monsoon climate, while the section in the Tibetan Plateau experiences an alpine climate. The total elevation drop from the source to the river mouth reaches 6,600 m, resulting in significant geographic and climatic differences across various regions. The average annual precipitation is 1067 mm, with temperatures ranging from -14 to 10 °C in January and from 14 to 32 °C in July.

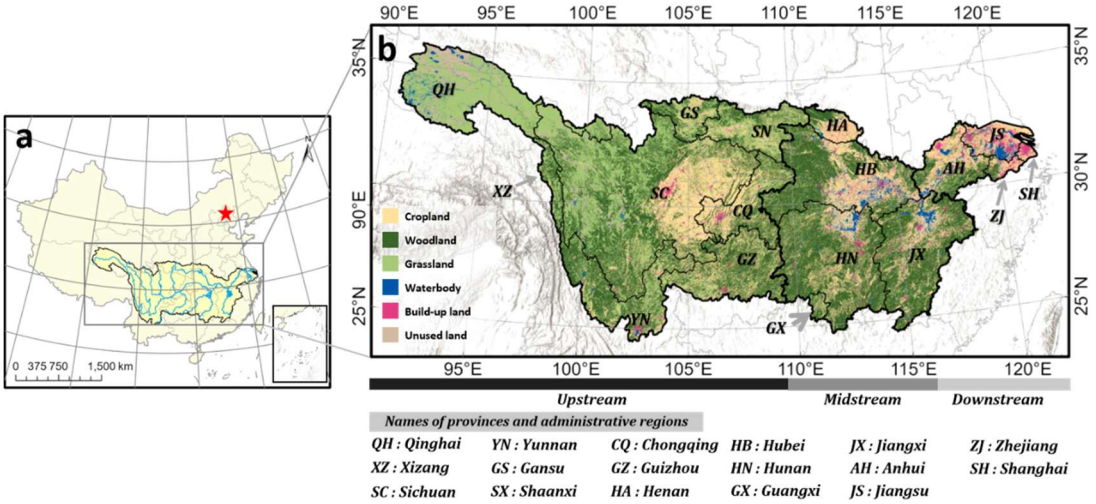


Fig. 1. Study Area: (a) Geographic location of the Yangtze River Basin. (b) Land use/cover status and regional division of the Yangtze River Basin in 2020.

2.2. Data sources

This study utilizes the China Multi-Period Land Use/Cover Remote Sensing Monitoring Database (CNLUCC) from the Institute of Geographic Sciences and Natural Resources Research, Chinese Academy of Sciences. The land use/cover data for 1980 primarily relies on Landsat-MSS remote sensing imagery, while data for 1990, 1995, 2000, 2005, and 2010 mainly use Landsat-TM/ETM imagery. For 2015 and 2020, Landsat 8 remote sensing imagery is predominantly used. The data were generated through manual visual interpretation, with a spatial resolution of 30 meters and a temporal resolution of one year. The classification system employs a two-level classification:

the first level includes cropland, woodland, grassland, waterbody, built-up land, and unused land; the second level consists of 25 classifications based on the natural attributes of land resources. Annual average temperature and annual precipitation data are based on meteorological data from over 2,400 stations in China. The spatial interpolation of meteorological data was generated using the Anusplin interpolation software based on calculated meteorological elements, resulting in a spatial interpolation dataset with a resolution of 1 km. Population and GDP data were derived from county-level population statistics and county-level GDP statistics in China. By calculating the distribution weights of land use types, nighttime light intensity, and settlement density, spatialization of population and GDP was conducted using raster spatial calculations, resulting in raster data with a spatial resolution of 1 km and a temporal resolution of one year. All data were sourced from the Resource and Environment Data Cloud Platform of CAS (REDCP) (http://www.resdc.cn). The DEM data is sourced from the NASA DEM published by the National Aeronautics and Space Administration (NASA), with a spatial resolution of 30 meters. Slope data were generated from the DEM data through slope analysis using ArcGIS software. The division of the basin into upstream, midstream, and downstream sections was based on provincial administrative boundaries and the spatial pattern of elevation change. Detailed data information is provided in Table 1.

Table 1 Resolution, Selected Years, and Sources of Data for This Study

Databases	Spatial resolution	Selected years	Data sources
Land use/cover	30m	1980,1990,1995,2000, 2005,2010,2015,2020	REDCP
Average annual	1km	1990,2000,2010,2020	

temperature			
Annual precipitation	1km	1990,2000,2010,2020	
population	1km	1995,2000,2010,2020	
GDP	1km	1995,2000,2010,2020	
DEM	30m	/	NASA
Slope	30m	/	/

Note: Considering the temporal inconsistency among the datasets, the population and GDP data from 1995 are approximated as the data for 1990 for the analysis.

2.3. Analytical methods

2.3.1. Analysis Model of Land Use Change

Transfer matrix analysis method reflects the spatiotemporal change characteristics of various land types at the beginning and end of a specified period within a given region(Zhu and Li 2003). It not only quantifies the conversion processes between different land types but also identifies the hotspot types involved in land conversion.

$$T = (T_{ij}) = \begin{bmatrix} T_{11} & T_{12} & \cdots & T_{1(n-1)} & T_{1n} \\ T_{21} & T_{22} & \cdots & T_{2(n-1)} & T_{2n} \\ \vdots & \vdots & \ddots & \vdots & \vdots \\ T_{n1} & T_{n2} & \cdots & T_{n(n-1)} & T_{nn} \end{bmatrix} \quad (1)$$

where T represents the land use/cover transition matrix; n represents the number of land use/cover types; i and j represent the land use types at the beginning and end of the study period, respectively; T_{ij} represents the land use/cover transition from type i to j.

Transitional change index refers to the proportion of area where land use in the region has undergone multiple transitions during the study period and eventually reverted to the initial land use type, and is an indicator of the instability of LUCC in the region. The land change probability index

represents the proportion of the area of the region that has undergone land-use change during the study period and is used to distinguish between sensitive areas of land-use change in the study area. The land use/cover change frequency index is quantified by counting the total instances of LUCC within a specified area during the study period, representing the activity level of LUCC in the region.

$$T_c = \frac{A_T}{A} \tag{2}$$

$$L_p = \frac{A_C}{A} \tag{3}$$

$$L_F = \sum_{i=1}^{n} \mathrm{N}_i \tag{4}$$

Where T_c denotes the Transitional Change Index, L_p represents the Land Change Probability Index, and L_F is the Land Use/Cover Change Frequency Index; A refers to the area of a given study region, A_T is the area where land use/cover type remained unchanged between the start and end years of the study period but experienced changes at some point during the study period; A_C is the total area that underwent LUCC throughout the study period; i denotes the different study periods, where i =1,2,…,7; and N_i is the area that experienced LUCC during the i-th period.

The land use/cover change composite index simultaneously characterizes both the frequency of LUCC and the proportional area affected, providing a metric for assessing the overall level of LUCC in the region, which aids in distinguishing the varying degrees of difficulty in LUCC across different areas of the watershed. The formula is as follows:

$$\mathrm{C} = L_p \times L_F \tag{5}$$

2.3.2. Driving force analysis

The GeoDetector was utilized to investigate the driving factors behind LUCC in the Yangtze River Basin from 1990 to 2020 (Wang et al. 2010). The grid cell size and variable partitioning methods in this study followed the MAUP verification process outlined by Zhou et al. (2020),

employing a grid size of 20 km × 20 km. GeoDetector consists of four modules: the factor detector, risk detector, interaction detector, and ecological detector. The factor detector employs the construction of the q statistic to represent the driving force of independent variables on dependent variables, with values ranging between 0 and 1. A higher q value indicates a stronger influence of the independent variable on the dependent variable. In this context, changes in land use types serve as the dependent variable, while elevation, slope, temperature, precipitation, GDP, and population are considered independent variables. Based on the temporal scale of population and GDP data, the driving force analysis is divided into three periods: 1990-2000, 2000-2010, and 2010-2020. The interaction detector quantitatively identifies the interactions between two factors, determining whether they act independently or if their joint effect is synergistic or antagonistic (Ju et al. 2016).

$$q = 1 - \frac{1}{N\sigma^2}\sum_{h=1}^{L} N_h \sigma_h^2 \quad (6)$$

Where h= 1, 2, …, L represents the level of independent variables; N_h represents denotes the number of grid cells in layer h; N represents the total number of grid cells in the region, σ_h^2 and σ^2 represent the variances of transition areas of a particular land type at level h and across the entire region, respectively.

2.3.3. Ecological Risk Assessment Model

The Ecological Risk Index (ERI) is employed to describe the extent of ecological loss in a region. The study area is partitioned into 3,158 grid cells, each measuring 25 km × 25 km, using an equal interval sampling method, and the ecological risk index value for each sampling cell is calculated based on the area proportions of various land use types within those cells. By calculating the ecological risk index, regional ecological losses can be quantified, clarifying the spatiotemporal differences in ecological risk. The calculation formula is as follows:

$$R_E = \sum_1^n \frac{A_i \times W_i}{A} \quad (7)$$

where R_E represents the ecological risk index, n represents the number of land use/cover types, A_i represents the total area of land use type i within the sampling area, W_i represents the ecological risk index reflected by land use type i, and A is the total area of the sampling region.

The hierarchical analysis method (AHP) was employed to determine the W_i of different land use types, considering the ecological sensitivity and degree of disturbance associated with each type(Zhou et al. 2014). A pairwise comparison matrix was constructed according to the Saaty 1–9 scale, systematically assessing the relative importance among land use types. After normalizing the matrix and calculating the maximum eigenvalue, a consistency check was performed to ensure the reliability of the judgments. The consistency ratio (CR) was calculated as 0.017 (<0.1), indicating good consistency. Consequently, the final weights were assigned as follows: cropland (0.192), woodland (0.056), grassland (0.087), waterbody (0.068), built-up land (0.481), and unused land (0.115).

Based on the results of the ecological risk index calculation, the data were standardized and ecological risk levels were classified using the density segmentation method. The regions with varying ecological risk were divided into five categories: low-risk areas (<0.3), relatively-low-risk areas (0.3–0.5), medium-risk areas (0.5–0.6), relatively-high-risk areas (0.6–0.7), and high-risk areas (>0.7).

3. Results and discussion

3.1. Temporal differences of LUCC in the Yangtze River Basin

LUCC in the Yangtze River Basin exhibited distinct temporal differences (Fig. 2). Overall, cropland, unused land, and grassland showed a decreasing trend, while built-up land and waterbody

areas increased significantly. Woodland experienced a fluctuating upward trend. Notably, there was a marked difference in the intensity of LUCC before and after 2000. During 1980–2000, changes in land use types were relatively moderate, with the area of waterbodies increasing by approximately 3.0×10^3 km², representing the most substantial change during this period. From 2000 to 2020, LUCC became much more pronounced. Cropland loss accelerated, with the reduction rate reaching 2.9 times that before 2000. Between 2000 and 2010, woodland area increased by approximately 1.1×10^4 km², primarily in the midstream and upstream regions, which significantly contributed to slowing deforestation(Han et al. 2021). The expansion rate of built-up land reached 1.2×10^3 km² per year, four times the rate observed in the previous two decades, and was mainly concentrated in downstream plain areas. Grassland and unused land also declined considerably. The total reduction in unused land over the 40-year period was approximately 1.1×10^4 km², with more than 95% of the loss occurring between 2000 and 2010. The reduction mainly resulted from woodland expansion into previously unused land in upstream areas.

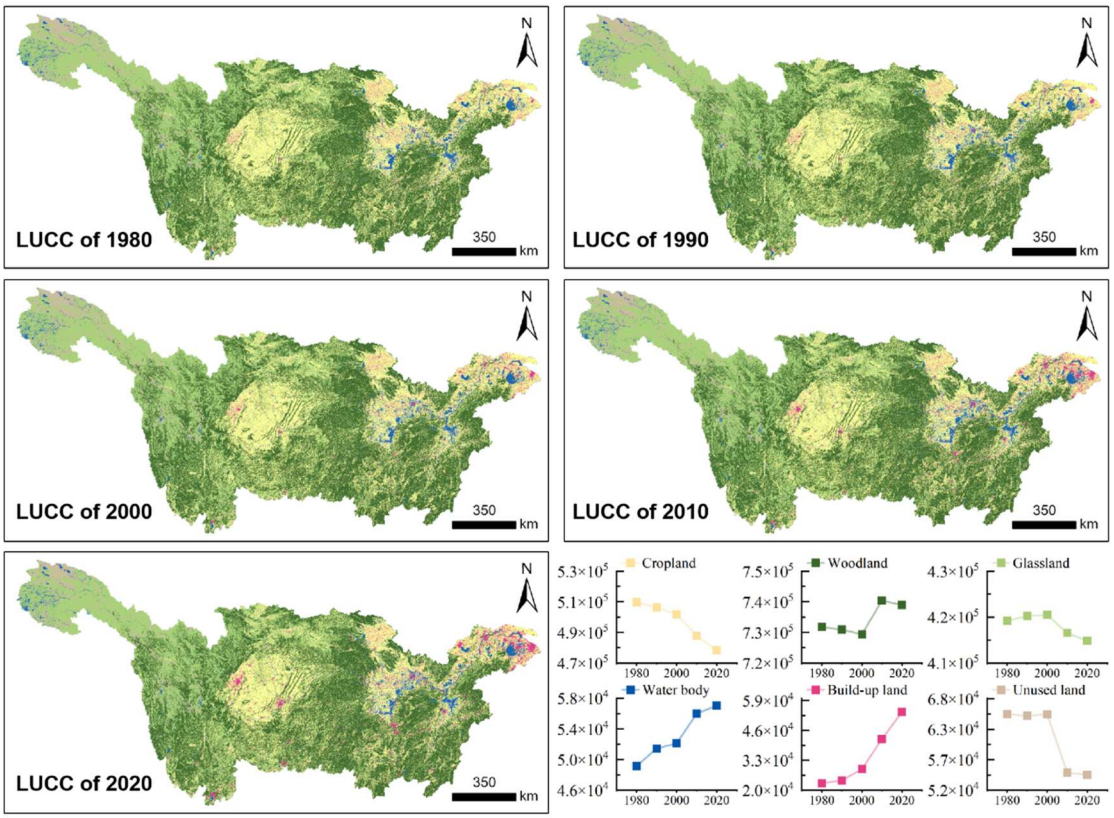


Fig. 2. Land use/cover distribution and area changes in the Yangtze River Basin from 1980 to 2020

A break point exists in the LUCC within the Yangtze River Basin, with the year 2000 dividing the process into a stable phase and an active phase (Fig. 3). Since 2000, LUCC in the basin have intensified markedly, primarily driven by a combination of policy interventions, economic growth, and demographic pressure(Liu et al. 2003, Yuan et al. 2023). Key contributing factors include the implementation of large-scale ecological engineering programs, the adoption of national development strategies, and the rapid acceleration of industrialization and urbanization(Kong et al. 2018, Han et al. 2021, Song et al. 2021). Over the past forty years, the primary LUCC in the basin have been characterized by the reciprocal conversion between cropland and woodland, the transformation between woodland and grassland, and the conversion of cropland into build-up land. During the stable phase, build-up land exhibited the most significant changes among all land use

types, while the increase in other types ranged from -1.55% to 5.83%. Specifically, the areas of cropland and woodland decreased, whereas grassland, waterbody, and build-up land increased, with unused land remaining essentially unchanged. From 1990 to 2000, approximately 4.5×10^3 km^2 of cropland was converted to build-up land, predominantly occurring in the Yangtze River estuary region, representing the most pronounced LUCC during the stable phase (Gellrich et al. 2007, Næss et al. 2021). In the active phase, LUCC exhibited significant fluctuations, with a total of 7.9×10^4 km^2 undergoing transformations, which is 3.82 times the total area transformed during the stable phase. Among these changes, build-up land and unused land exhibited the most significant shifts, with an increase of 2.5×10^4 km^2 in build-up land during the active phase, which is 4.1 times the increase observed in the stable phase. The reduction in unused land occurred almost entirely during the active phase, primarily reflected in the conversion of unused land to grassland in the Qinghai and Xizang regions. Between 2000 and 2010, 1.7×10^4 km^2 of grassland was converted into cropland, 1.2×10^3 km^2 of unused land was converted into grassland, and 1.2×10^4 km^2 of grassland was converted into build-up land, with these LUCC primarily being unidirectional. From 2010 to 2020, the conversion of land types intensified, with 1.3×10^4 km^2 of cropland converted to residential land. The mutual conversion between cropland and woodland, as well as between woodland and grassland, became more frequent, primarily occurring in the upper and middle regions of the basin, such as Sichuan, Chongqing and Hubei. The conversion of cropland to grassland and forest is due to the implementation of relevant ecological conservation policies (e.g., GFG program) in China (Long et al. 2007, Serra et al. 2008, Wang et al. 2012).

Further analysis of LUCC for each period indicates that transitional changes occur relatively frequently. Transitional changes refer to land use that reverts to its original state after temporary

transformation and accounted for over 70 percent of total LUCC events. Among all land types, grassland exhibited the highest frequency of such fluctuations, with an area of 3 km², while unused land showed the greatest instability, with a 93 percent reversion rate. In contrast, the transition probability for built-up land was only 17 percent, reflecting its strong irreversibility.

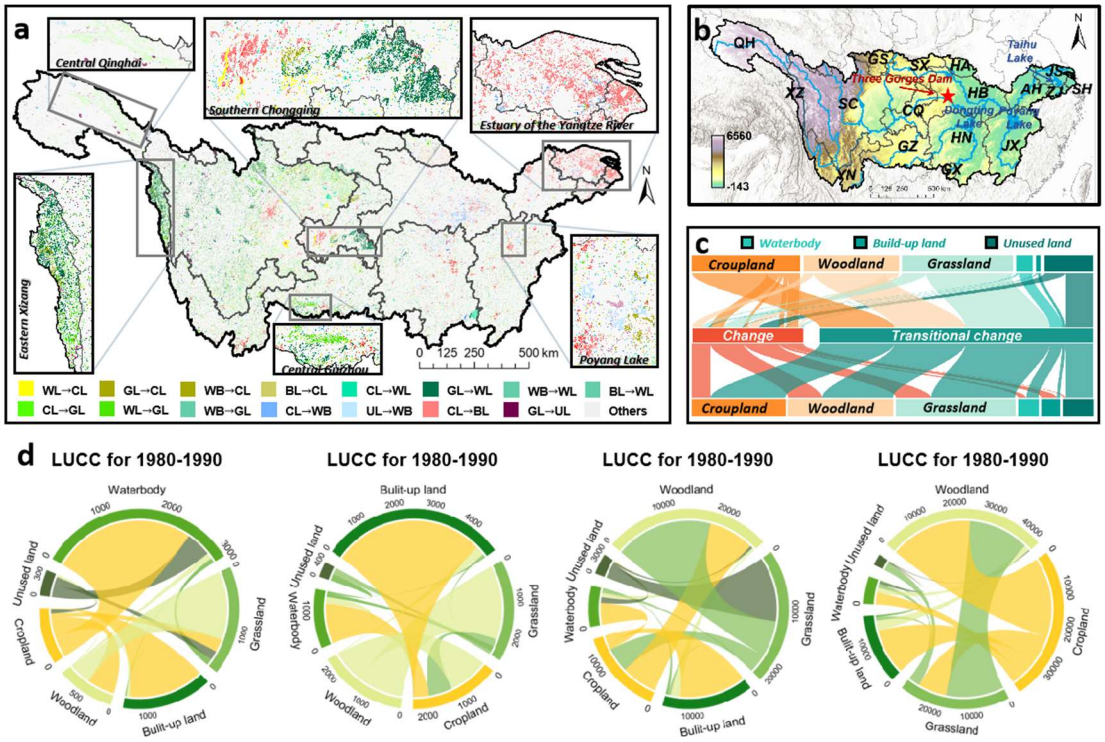


Fig. 3. LUCC in the Yangtze River Basin from 1980 to 2020: (a) Overall land transfer situation in the Yangtze River Basin from 1980 to 2020. (b) Distribution of the main stem and tributaries of the Yangtze River, large lakes, and provinces within the basin. (c) Transitional changes in land use/cover within the Yangtze River Basin. (d) LUCC in the Yangtze River Basin during the periods of 1980-1990, 1990-2000, 2000-2010, and 2010-2020.

3.2. Spatial Characteristics of LUCC in the Yangtze River Basin

The spatial characteristics of LUCC in the Yangtze River Basin are illustrated in Fig. 4. Compared to other regions, LUCC in the upstream region of the Yangtze River Basin shows more pronounced features. The downstream region has mainly experienced extensive built-up land

266 expansion. In the midstream area, significant increases in waterbodies have occurred due to
267 aquaculture growth, while cropland and woodland changes dominate in the upstream region. These
268 spatial transformations reflect both ecological restoration in high-altitude regions and climate-
269 induced hydrological shifts, such as snowmelt lake formation due to glacier retreat on the Tibetan
270 Plateau.

271 Between 1980 and 2020, land change patterns were quite complex, with certain areas
272 experiencing frequent temporary changes during the study period. This situation was predominantly
273 observed along the main stem of the Yangtze River and its secondary tributaries, particularly in
274 high-altitude and water source areas, where the transitional change index (calculated using Equation
275 2) can reach up to 0.8. This indicates that regions close to large water bodies or those at relatively
276 high elevations are more likely to undergo temporary land changes, leading to greater instability in
277 land structure. Analysis of the probability of land use change (based on Equation 3) in various
278 regions of the basin from 1980 to 2020 shows that the upper reaches are more active. Regions with
279 a higher proportion of land change are mainly distributed in Xizang, eastern Sichuan, eastern
280 Chongqing, and Shanghai, with the highest change proportion in Xizang reaching 89.4%.
281 Considering the presence of transitional changes in Xizang, it indicates that the land in this area has
282 likely undergone at least one change. By calculating the differences in land use change frequency
283 (based on Equation 4) across different regions of the basin over five-year intervals (with the period
284 from 1980 to 1990 counted as ten years), it is found that the upper reaches exhibit more frequent
285 changes. About 20% of the area has undergone land-use change over 40 years, and the area with
286 more than two changes amounts to 1.4×10^5 km^2. The most active regions for change in the upper
287 reaches are located in northern Qinghai, Xizang, and eastern Sichuan, with high change frequency

concentrated in these areas. In contrast, regions with higher change frequencies in the middle and lower reaches are mainly found around the main stem of the Yangtze River and large lakes.

The analysis of LUCC using a comprehensive index (based on Equation 5) reveals that Xizang is the area within the basin most prone to LUCC, with a comprehensive index of 1.81 and high frequency and area of changes. Henan and Shanghai are regions in the middle and lower reaches with relatively high comprehensive indices, primarily driven by increases in built-up land, with indices of 0.67 and 0.51, respectively. Other regions exhibit relatively few occurrences of simultaneous high-frequency and large-area LUCC. Overall, the upper reaches are more susceptible to land changes compared to the middle and lower reaches, with larger areas and higher frequencies of LUCC occurring in the upper reaches. Aside from some densely populated areas in the middle and lower reaches leading to increases in built-up land, the comprehensive index for the upper reaches is generally higher than that of the middle and lower reaches, indicating a close relationship between the difficulty of land change and geographical factors.

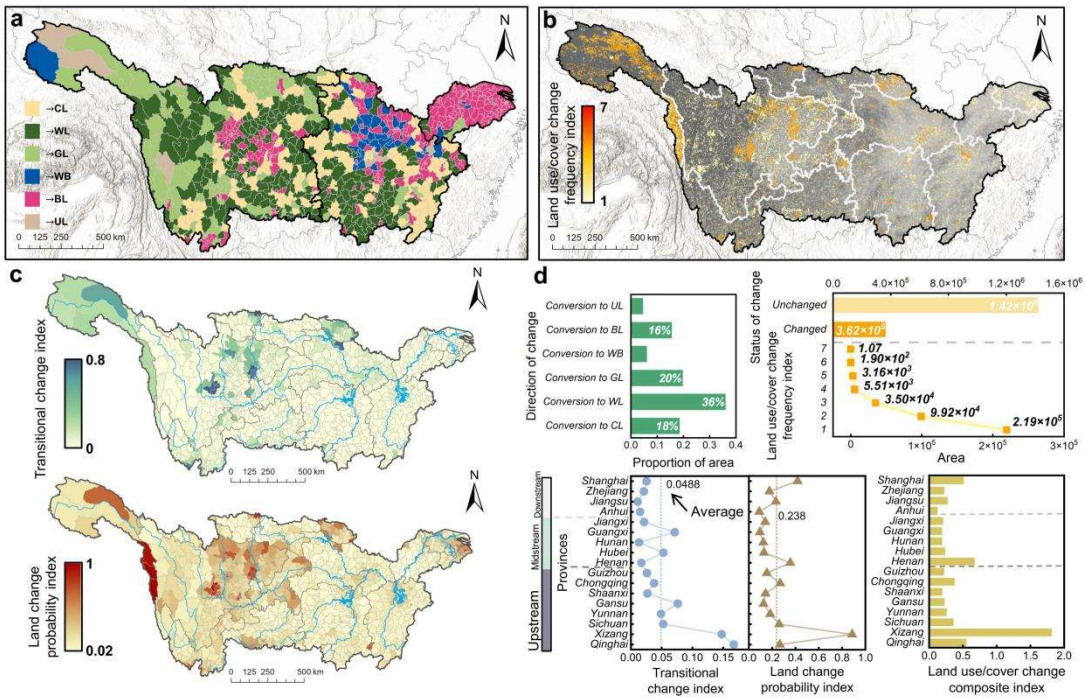


Fig. 4. Spatial Characteristics of Land Change in the Yangtze River Basin: (a) Main types of land change directions in different regions of the Yangtze River Basin. (b) The land use/cover change frequency index from 1980 to 2020, covering eight study years, with a maximum of seven recorded changes. (c) Transitional change index and land change probability index within the basin from 1980 to 2000. (d) Detailed data from the above figures and the land use change comprehensive index in the Yangtze River Basin from 1980 to 2020.

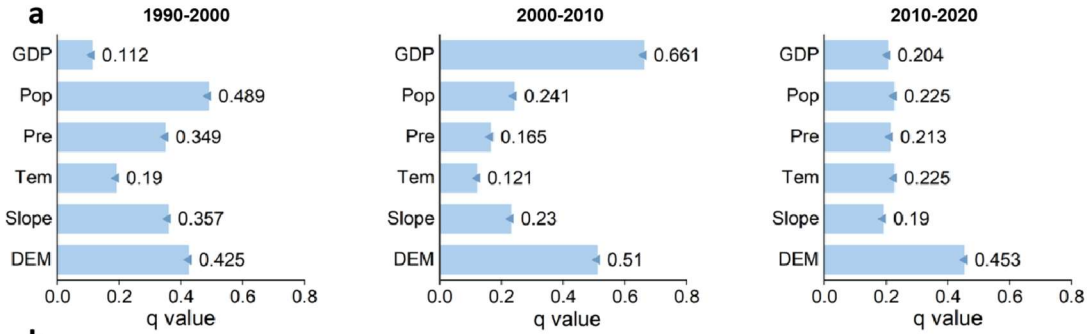
3.3. Driving Factors of Land Use Change

The factor detection results indicate that the LUCC in the basin is shifting from being driven by socio-economic factors to geographic factors (Fig. 5). Elevation has a significant impact on land changes during all three periods, with q statistics of 0.452, 0.510, and 0.453, ranking second in the 1990-2010 period and first in the 2010-2020 period. This is primarily because land use intensity in high-altitude areas is lower, making it easier for land to be developed. In contrast, low-altitude areas are predominantly composed of cropland, woodland, and build-up land, which have lower convertibility. Rainfall and temperature, as climate factors, have a certain impact on land use; among these, Pre has a relatively minor influence on LUCC, ranking fourth, fifth, and fourth in influence weight during each period, while the impact of Tem on LUCC has been increasing year by year, with q factors of 0.190, 0.121, and 0.225. This may be due to the construction of water conservancy projects, which makes the distribution of water resources subject to human control, resulting in an indirect influence on LUCC that is less significant than the direct impact of Tem. Population and GDP are the main driving factors for land use type changes in the 1990-2000 and 2000-2010 periods, respectively. Pop has the highest q statistic in the 1990-2000 period, reaching 0.489, ranking as the second driving factor for that period, and ranking third in the 2000-2020 period, indicating that

population is one of the main driving forces behind LUCC. GDP, in addition to reflecting the development level of the region, is also related to urban characteristics, which leads to less obvious direct impacts on land use conversion, causing fluctuations in the q statistic of GDP across periods.

By calculating the interaction strength among the six target factors of LUCC across three periods, it was found that socioeconomic, climatic, and geographic factors collectively drive LUCC in the Yangtze River Basin. During the 1990-2000 period, interactions between Tem and DEM, as well as population, exhibited bilinear enhancement, while interactions between other factors showed nonlinear enhancement. In the 2000-2010 period, the interactions between Tem and slope, as well as population, were also bilinear, with the rest remaining nonlinear. From 2010 to 2020, interactions between population and Tem, Pre, and GDP, as well as between slope and these same factors, continued to show bilinear enhancement, while the rest were nonlinear. Over time, the interactions among the factors increasingly demonstrated bilinear enhancement, suggesting that the combined effects of various factors have strengthened their influence on LUCC, indicating the existence of coupling effects among them.

a



b

	DEM	Slope	Tem	Pre	Pop	GDP	DEM	Slope	Tem	Pre	Pop	GDP	DEM	Slope	Tem	Pre	Pop	GDP
	1990-2000						2000-2010						2010-2020					
DEM	0.425						0.510						0.453					
Slope	0.890	0.357					0.584	0.230					0.520	0.190				
Tem	0.997	0.561	0.190				0.551	0.511	0.121				0.776	0.841	0.225			
Pre	0.890	0.492	0.585	0.349			0.551	0.367	0.411	0.165			0.754	0.823	0.465	0.213		
Pop	0.997	0.545	0.554	0.597	0.489		0.817	0.369	0.697	0.305	0.241		0.502	0.315	0.728	0.665	0.225	
GDP	0.653	0.462	0.607	0.570	0.601	0.112	0.802	0.815	0.781	0.689	0.817	0.661	0.626	0.618	0.371	0.372	0.629	0.204

Fig. 5. Analysis of the Driving Factors of LUCC in the Yangtze River Basin and Interaction Monitoring Results: (a) The q values of each variable during different periods. (b) The interaction detection results of each variable, where the orange sections indicate a bilinear enhancement between two independent variables, and the rest indicate nonlinear enhancement.

Further analysis of the results from the factor detector and interaction detector reveals that before 2010, the variables with the highest q statistics were Pop and GDP. Geographical, climatic, and social factors act as three independent influencing elements driving land changes in the basin. During the period from 2010 to 2020, the q statistics for factors other than geographical factors showed a reduced gap, and the interactions exhibited a trend of bilinear enhancement. This indicates that the factors are increasingly coupled to jointly drive the transformation of land use in the basin. These findings align with previous studies identifying socio-economic factors as dominant LUCC drivers before 2010. For instance, Liu et al. (2003) demonstrated that China's LUCC in the 1990s was primarily driven by economic expansion and population growth. However, our results reveal a shift after 2010, with geographic and climatic factors—especially elevation and temperature—playing increasingly influential roles. This transition in dominant drivers supports Zhou et al. (2020), who reported that social and economic development is the main driving force for the expansion of built-up areas, and geographical differentiation is the leading factor for the transformation of cultivated land, forest land and grassland. This change is due to the fact that before 2000, the primary form of land change was the conversion of productive land to built-up land, with the expansion of built-up land primarily determined by economic factors and less influenced by climate change. After 2000, the mutual conversion among different land types began to increase, with a series of measures such as returning farmland to forest and grassland complicating land conversion types. The main

driving forces behind LUCC gradually shifted from socioeconomic factors to a combination of geographical, climatic, and social factors. After 2010, as land in various regions became fully developed and most of the suitable land had already been utilized, geographic factors, as constraints on land development, began to dominate the process of LUCC in the Yangtze River Basin. Our interaction detection further suggests that the strengthening bilinear enhancement effects among natural and human factors indicate an increasingly complex and coupled LUCC mechanism in the basin.

3.4. Spatial and Temporal Changes of Risks in the Yangtze River Basin

The ecological risk in the Yangtze River Basin shows significant spatial and temporal changes, with an overall decreasing trend in the upstream regions. As shown in Fig. 6, the distribution of ecological risk levels in the basin is highly influenced by geographical factors. A spatial autocorrelation analysis of ecological risk changes over the past 40 years reveals a positive spatial autocorrelation in ecological risk changes within the basin, with a Moran's I index of 0.13 and a z-value of 10.3. Areas above the Hu line show a year-on-year reduction in ecological risk, primarily due to the conversion of unused land to grassland in the Qinghai region. In contrast, some areas below the Hu line, particularly in the Sichuan Basin, the urban agglomerations in the middle and lower reaches, and the Yangtze River estuary, exhibit a significant increase in ecological risk(Liu et al. 2014). By identifying key areas of ecological risk change in the basin, it is evident that ecological risk in the Qinghai region has significantly decreased after 2000, with reduced risk disparities among different areas. Conversely, ecological risk has slightly increased in the Sichuan Basin and the Mid-Basin Urban Agglomeration. The development of the economy and the continuous expansion of

built-up land have resulted in an upward trend in ecological risk in the Yangtze River Estuary over the past 40 years, widening the ecological risk gap between regions.

Due to LUCC, the area of high-risk zones in the basin has gradually increased, exhibiting regional effects. Over the past 40 years, high-risk areas have increased by a total of 1.1×10^3 km^2, representing an 18.09% increase. The area of relatively-high-risk zones has seen the most significant growth (1.4 times), increasing by 7.3×10^3 km^2. The area of moderate-risk zones has increased by 1.5×10^4 km^2, reflecting a growth rate of 51.4%. Meanwhile, the proportion of low-risk areas has decreased from 79.64% in 1980 to 77.93% in 2020, with a reduction of up to 3.2×10^4 km^2. Cropland, built-up land, and unused land are regions of higher ecological risk. The observed increase in high-risk areas and compression of low-risk zones aligns with previous findings. Liu et al. (2019) identified heightened ecological risks in the Yangtze River Delta and midstream urban clusters due to urban expansion. Our results corroborate these patterns, particularly in the Sichuan Basin and the Yangtze Estuary. However, unlike earlier studies that primarily focused on downstream regions, we found a pronounced reduction in ecological risk in upstream areas, especially in Qinghai, driven by ecological restoration policies and land conversion from unused land to grassland. This spatial divergence highlights the heterogeneous ecological responses to LUCC across the basin. Furthermore, our assessment of transitional changes adds a new dimension to risk analysis: areas dominated by unstable LUCC types—such as grassland and unused land—tend to experience greater ecological volatility, whereas built-up land, due to its irreversible nature (only 17% transition probability), contributes to long-term ecological pressure. These findings emphasize the importance of incorporating land conversion stability and reversibility into future ecological risk assessments and policy interventions.

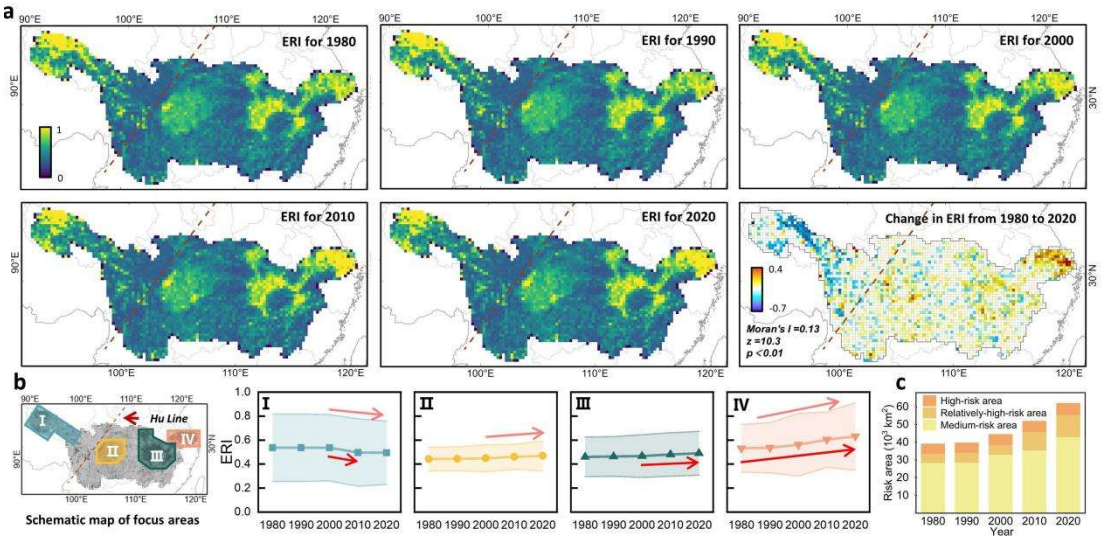


Fig. 6. Ecological risk distribution in the Yangtze River Basin: (a) ERI distribution for each period in the Yangtze River Basin and the changes in ERI from 1980 to 2020. (b) ERI of focus areas in the basin during each period: Qinghai region (I), Sichuan Basin (II), Mid-Basin Urban Agglomeration (III), Yangtze River Estuary (IV). (c) The area of medium- and higher-risk regions in each period.

4. Conclusion

In the context of rapid urbanization and exacerbating climate change, this study employed methods such as the geographic detector model and ecological risk model to reveal the evolution process, driving forces, and ecological risk characteristics of LUCC in the Yangtze River Basin. The results show that over the past forty years, cropland has been continuously converted into build-up land, with approximately 80% of the 35,000 km² increase in build-up land originating from the occupation of cropland. Since 2000, the frequency of conversions among cropland, woodland, and grassland has significantly increased, and 70% of LUCC in the basin over the past four decades has been identified as transitional changes. LUCC in the basin have begun to shift toward being jointly driven by geographical, climatic, and social factors. Over the past forty years, the area experiencing

increased ecological risk has reached 31,000 km², while the area of low-risk zones has declined to its minimum. Low-risk areas have been compressed by high-risk areas, pushing the basin's ecological system toward extremization.

Data availability

Data sets generated during the current study are available from the corresponding author on reasonable request.

References

Bayer, A.D., Lindeskog, M., Pugh, T.A.M., Anthoni, P.M., Fuchs, R. and Arneth, A. (2017) Uncertainties in the land-use flux resulting from land-use change reconstructions and gross land transitions. Earth System Dynamics 8(1), 91-111.

Bryan, B.A., Gao, L., Ye, Y., Sun, X., Connor, J.D., Crossman, N.D., Stafford-Smith, M., Wu, J., He, C., Yu, D., Liu, Z., Li, A., Huang, Q., Ren, H., Deng, X., Zheng, H., Niu, J., Han, G. and Hou, X. (2018) China's response to a national land-system sustainability emergency. Nature 559(7713), 193-204.

Chen, C., Park, T., Wang, X., Piao, S., Xu, B., Chaturvedi, R.K., Fuchs, R., Brovkin, V., Ciais, P., Fensholt, R., Tommervik, H., Bala, G., Zhu, Z., Nemani, R.R. and Myneni, R.B. (2019) China and India lead in greening of the world through land-use management. Nature Sustainability 2(2), 122-129.

Chen, X.L., Zhao, H.M., Li, P.X. and Yin, Z.Y. (2006) Remote sensing image-based analysis of the relationship between urban heat island and land use/cover changes. Remote Sensing of Environment 104(2), 133-146.

Deng, J.S., Wang, K., Hong, Y. and Qi, J.G. (2009) Spatio-temporal dynamics and evolution of land use change and landscape pattern in response to rapid urbanization. Landscape and Urban Planning 92(3-4), 187-198.

Feng, X.M., Fu, B.J., Piao, S., Wang, S.H., Ciais, P., Zeng, Z.Z., Lü, Y.H., Zeng, Y., Li, Y., Jiang, X.H. and Wu, B.F. (2016) Revegetation in China's Loess Plateau is approaching sustainable water resource limits. Nature Climate Change 6(11), 1019-+.

Gao, J. and Liu, Y.S. (2011) Climate warming and land use change in Heilongjiang Province, Northeast China. Applied Geography 31(2), 476-482.

Gellrich, M., Baur, P., Koch, B. and Zimmermann, N.E. (2007) Agricultural land abandonment and natural forest re-growth in the Swiss mountains: A spatially explicit economic analysis. Agriculture Ecosystems & Environment 118(1-4), 93-108.

Han, Y., Ma, Z., Li, M. and Chen, L. (2021) Numerical Simulation of the Impact of Land Use/Cover Change on Land Surface Process in China from 2001 to 2010. Climatic and Environmental Research 26(1), 75-90.

He, L., Li, W., Tian, S. and Zheng, H. (2018) Analysis of the impact of rapid urbanization on farmland protection in the Yangtze River Economic Belt. Acta Ecologica Sinica 38(21), 7782-7789.

Jiang, L., Deng, X.Z. and Seto, K.C. (2012) Multi-level modeling of urban expansion and cultivated land conversion for urban hotspot counties in China. Landscape and Urban Planning 108(2-4), 131-139.

Jing, Q., He, J., Li, Y., Yang, X., Peng, Y., Wang, H., Yu, F., Wu, J., Gong, S., Che, H. and Zhang, X. (2024) Analysis of the spatiotemporal changes in global land cover from 2001 to 2020. SCIENCE OF THE TOTAL ENVIRONMENT 908.

Ju, H.R., Zhang, Z.X., Zuo, L.J., Wang, J.F., Zhang, S.R., Wang, X. and Zhao, X.L. (2016) Driving forces and their interactions of built-up land expansion based on the geographical detector - a case study of Beijing, China. International Journal of Geographical Information Science 30(11), 2188-2207.

Kong, L., Wu, T., Xiao, Y., Xu, W., Zhang, X., Daily, G.C. and Ouyang, Z. (2023) Natural capital investments in China undermined by reclamation for cropland. Nature Ecology & Evolution 7(11), 1771-1777.

Kong, L., Zhang, L., Zheng, H., Xu, W., Xiao, Y. and Ouyang, Z. (2018) Driving forces behind ecosystem spatial changes in the Yangtze River Basin. Acta Ecologica Sinica 38(3), 741-749.

Kong, X.S., Fu, M.X., Zhao, X., Wang, J. and Jiang, P. (2022) Ecological effects of land-use change on two sides of the Hu Huanyong Line in China. Land Use Policy 113.

Lambin, E.F. and Meyfroidt, P. (2011) Global land use change, economic globalization, and the looming land scarcity. Proc Natl Acad Sci U S A 108(9), 3465-3472.

Lawler, J.J., Lewis, D.J., Nelson, E., Plantinga, A.J., Polasky, S., Withey, J.C., Helmers, D.P., Martinuzzi, S., Pennington, D. and Radeloff, V.C. (2014) Projected land-use change impacts on ecosystem services in the United States. Proc Natl Acad Sci U S A 111(20), 7492-7497.

Liu, G., Zhang, L. and Zhang, Q. (2014) Spatial and temporal dynamics of land use and its influence on ecosystem service value in Yangtze River Delta. Acta Ecologica Sinica 34(12), 3311-3319.

Liu, J., Zhang, Z., Zhuang, D., Wang, Y., Zhou, W., Zhang, S., Li, R., Jiang, N. and Wu, S. (2003) A study on the spatial temporal dynamic changes of land use and driving forces analyses of China in the 1990s. Geographical Research 22(1), 1-12.

Liu, J.Y., Zhang, Z.X., Xu, X.L., Kuang, W.H., Zhou, W.C., Zhang, S.W., Li, R.D., Yan, C.Z., Yu, D.S., Wu, S.X. and Nan, J. (2010) Spatial patterns and driving forces of land use change in China during the early 21st century. Journal of Geographical Sciences 20(4), 483-494.

Liu, Y., Zhou, Y. and Du, Y. (2019) Study on the Spatio-Temporal Patterns of Habitat Quality and Its Terrain Gradient Effects of the Middle of the Yangtze River Economic Belt Based on InVEST Model. Resources and Environment in the Yangtze Basin 28(10), 2429-2440.

Liu, Y.L., Luo, T., Liu, Z.Q., Kong, X.S., Li, J.W. and Tan, R.H. (2015) A comparative analysis of urban and rural construction land use change and driving forces: Implications for urban-rural coordination development in Wuhan, Central China. Habitat International 47, 113-125.

Long, H., Tang, G., Li, X. and Heilig, G.K. (2007) Socio-economic driving forces of land-use change in Kunshan, the Yangtze River Delta economic area of China. Journal of Environmental Management 83(3), 351-364.

Long, H.L. (2014) Land use policy in China: Introduction. Land Use Policy 40, 1-5.

Luyssaert, S., Jammet, M., Stoy, P.C., Estel, S., Pongratz, J., Ceschia, E., Churkina, G., Don, A., Erb, K., Ferlicoq, M., Gielen, B., Grünwald, T., Houghton, R.A., Klumpp, K., Knohl, A., Kolb, T., Kuemmerle, T., Laurila, T., Lohila, A., Loustau, D., McGrath, M.J., Meyfroidt, P., Moors, E.J., Naudts, K., Novick, K., Otto, J., Pilegaard, K., Pio, C.A., Rambal, S., Rebmann, C., Ryder, J., Suyker, A.E., Varlagin, A., Wattenbach, M. and Dolman, A.J. (2014) Land management and land-cover change have impacts of similar magnitude on surface temperature. Nature Climate Change 4(5), 389-393.

Montgomery, D.R. (2007) Soil erosion and agricultural sustainability. Proc Natl Acad Sci U S A 104(33), 13268-13272.

Næss, J.S., Cavalett, O. and Cherubini, F. (2021) The land-energy-water nexus of global bioenergy potentials from abandoned cropland. Nature Sustainability 4(6), 525-+.
Ning, J., Liu, J.Y., Kuang, W.H., Xu, X.L., Zhang, S.W., Yan, C.Z., Li, R.D., Wu, S.X., Hu, Y.F., Du, G.M., Chi, W.F., Pan, T. and Ning, J. (2018) Spatiotemporal patterns and characteristics of land-use change in China during 2010-2015. Journal of Geographical Sciences 28(5), 547-562.
Powers, R.P. and Jetz, W. (2019) Global habitat loss and extinction risk of terrestrial vertebrates under future land-use-change scenarios. Nature Climate Change 9(4), 323-+.
Serra, P., Pons, X. and Saurí, D. (2008) Land-cover and land-use change in a Mediterranean landscape:: A spatial analysis of driving forces integrating biophysical and human factors. Applied Geography 28(3), 189-209.
Seto, K.C. and Fragkias, M. (2005) Quantifying spatiotemporal patterns of urban land-use change in four cities of China with time series landscape metrics. Landscape Ecology 20(7), 871-888.
Song, K., Wang, Y. and Li, Y. (2021) Monitoring of ecological environment changes in the Yangtze River Economic Belt (Jiangsu province) from 1999 to 2020 and analysis of the driving forces of human activities. Bulletin of Surveying and Mapping (2), 7-12.
Song, X.P., Hansen, M.C., Stehman, S.V., Potapov, P.V., Tyukavina, A., Vermote, E.F. and Townshend, J.R. (2018) Global land change from 1982 to 2016. Nature 560(7720), 639-643.
Soroye, P., Newbold, T. and Kerr, J. (2020) Climate change contributes to widespread declines among bumble bees across continents. Science 367(6478), 685-+.
Vadrevu, K.P. and Ohara, T. (2020) Focus on land use cover changes and environmental impacts in South/Southeast Asia. ENVIRONMENTAL RESEARCH LETTERS 15(10).
van Asselen, S. and Verburg, P.H. (2013) Land cover change or land-use intensification: simulating land system change with a global-scale land change model. Glob Chang Biol 19(12), 3648-3667.
Wang, J., Chen, Y.Q., Shao, X.M., Zhang, Y.Y. and Cao, Y.G. (2012) Land-use changes and policy dimension driving forces in China: Present, trend and future. Land Use Policy 29(4), 737-749.
Wang, J.F., Li, X.H., Christakos, G., Liao, Y.L., Zhang, T., Gu, X. and Zheng, X.Y. (2010) Geographical Detectors-Based Health Risk Assessment and its Application in the Neural Tube Defects Study of the Heshun Region, China. International Journal of Geographical Information Science 24(1), 107-127.
Winkler, K., Fuchs, R., Rounsevell, M. and Herold, M. (2021) Global land use changes are four times greater than previously estimated. Nature Communications 12(1), 2501.
Wu, J.G. and Hobbs, R. (2002) Key issues and research priorities in landscape ecology: An idiosyncratic synthesis. Landscape Ecology 17(4), 355-365.
Yang, H., Zhou, H., Deng, S., Zhou, X. and Nie, S. (2024) Spatiotemporal Variation of Ecosystem Services Value and its Response to Land Use Change in the Yangtze River Basin, China. INTERNATIONAL JOURNAL OF ENVIRONMENTAL RESEARCH 18(2).
Yang, H.F., Mu, S.J. and Li, J.L. (2014) Effects of ecological restoration projects on land use and land cover change and its influences on territorial NPP in Xinjiang, China. Catena 115, 85-95.
Yang, H.F., Zhong, X.N., Deng, S.Q. and Xu, H. (2021) Assessment of the impact of LUCC on NPP and its influencing factors in the Yangtze River basin, China. Catena 206.
Yu, Z., Ciais, P., Piao, S., Houghton, R.A., Lu, C., Tian, H., Agathokleous, E., Kattel, G.R., Sitch, S., Goll, D., Yue, X., Walker, A., Friedlingstein, P., Jain, A.K., Liu, S. and Zhou, G. (2022) Forest expansion dominates China's land carbon sink since 1980. Nature Communications 13(1), 5374.
Yuan, X., Wang, C., Li, B., Wang, W. and Chen, N. (2023) Review of the Driving Forces and Impacts of Land Use/Cover Change in the Yangtze River Basin. Geomatics and Information Science of Wuhan

University 48(8), 1241-1255.
Zhou, D., Shi, P., Wu, X., Ma, J. and Liang, S. (2014) Urbanization spatial expansion and regional landscape ecological risk of Yantai City. Chinese Journal of Ecology 33(2), 477-485.
Zhou, Y., Li, X.H. and Liu, Y.S. (2020) Land use change and driving factors in rural China during the period 1995-2015. Land Use Policy 99.
Zhu, H. and Li, X. (2003) Discussion on the Index Method of Regional Land Use Change. Acta Geographica Sinica 58(5), 643-650.